Journal of Alloys and Compounds 509 (2011) 4617–4621

Contents lists available at ScienceDirect

Journal of Alloys and Compounds

journal homepage: www.elsevier.com/locate/jallcom

Effects of Sn-substitution on the microstructure and magnetic properties of Bi-CVG ferrite with low temperature sintering

Qi-Ming Xu [a], Ning Li [a,*], Wei-Bin Liu [a], Xiao-Gang Lu [b], Chang-Jie Gao [b], Yong-An Wang [c]

[a] School of Material Science and Engineering, Xi'an University of Architecture and Technology, Xi'an 710055, PR China
[b] Institute 206 of China Ordnance Industries Group Corporation, Xi'an 710100, PR China
[c] Shaanxi Jinshan Electronic Components Co., Ltd., Xian Yang 712021, PR China

ARTICLE INFO

Article history:
Received 10 October 2010
Received in revised form 16 January 2011
Accepted 19 January 2011
Available online 28 January 2011

Keywords:
Bi-CVG ferrite
Low temperature sintering
Magnetic property
Sn-substitution
Microstructure

ABSTRACT

$[Bi_{0.75}Y_{1.05-x}Ca_{1.2+x}](Fe_{4.4-x}Sn_xV_{0.6})O_{12}$ (Sn_x:Bi-CVG) ferrite materials were prepared by conventional ceramic technique. The bulk density, microstructure and the magnetic properties of the obtained samples were analyzed. The results showed that moderate addition of Sn^{4+} in Bi-CVG could lower the sintering temperature and enhance the soft magnetic properties obviously. With the increase of Sn^{4+} content, the saturation magnetization first increased and then decreased, while the coercivity and the ferromagnetic resonance linewidth (ΔH) first sharply decreased and then slightly increased. Additionally, the specimen of $[Bi_{0.75}Y_{0.65}Ca_{1.6}](Fe_{4.0}Sn_{0.4}V_{0.6})O_{12}$ sintered at 1075 °C possessed the highest density and the optimum magnetic properties: RD (the relative density) = 98.49%, H_c = 152.3 A/m, $4\pi M_s = 711.3 \times 10^{-4}$ T, ΔH = 2.1 kA/m.

1. Introduction

Yttrium iron garnet (YIG, $Y_3Fe_5O_{12}$) is a well-known ferrimagnetic material, which is assigned to a cubic structure (space group *Ia3d*), with eight $R_3Fe_5O_{12}$ molecules in each cell. Because of large ion radius, R^{3+} ion can occupy only dodecahedral sites, rather than octahedral and tetrahedral sites. In the case of ferrimagnetic garnet $R_3Fe_5O_{12}$, the ion distribution structure can be represented by the garnet formula as $\{R_3\}[Fe_2](Fe_3)O_{12}$, where { }, [ ], ( ) represent 24*c* (dodecahedral), 16*a* (octahedral) and 24*d* (tetrahedral) sites, respectively [1].

YIG and substituted YIG ceramic materials have been applied widely in the microwave devices, such as circulators, oscillators and phase shifters, due to their controllable saturation magnetization, low dielectric loss tangent ($\tan\delta$) in microwave region and small linewidth (ΔH) in ferromagnetic resonance [2–9]. High density and saturation magnetization, as well as uniform microstructure, are essential in these materials to minimize the energy loss at high frequencies [10]. However, in order to synthesize high-density YIG, a sintering temperature of > 1400 °C is usually required, which is higher than the melting points of high conductive metals like Ag–Pd alloy (1145 °C) [10,11]. Recently, it has been reported that the sintering temperature could be reduced from 1400 °C to 1280 °C for $CaO–V_2O_5$ doped YIG with a relative density of >97%. Subsequently, the sintering temperatures of YIG system were reduced to 1100 °C for $(Ca_{1.2}Y_{1.8})(V_{0.6}Fe_{4.4})O_{12}$ and $(Bi_{0.75}Ca_{1.2}Y_{1.05})(V_{0.6}Fe_{4.4})O_{12}$(Bi-CVG) [11–16]. However, the effects of some other additives are still to be investigated in an attempt to improve the density and magnetic properties of YIG materials at still lower sintering temperatures.

Our previous investigations showed that In-substituted Bi-CVG ceramics can be prepared at a lower temperature of 1075 °C [17]. But In_2O_3 is very expensive. In order to reduce the cost, in the present work, cheaper Sn was used instead of In. Sn-substituted Bi-CVG ceramics were prepared by conventional ceramic technique at low sintering temperature and their microstructures and magnetic properties were characterized.

2. Experimental

Polycrystalline samples of $[Y_{1.05-x}Bi_{0.75}Ca_{1.2+x}](Fe_{4.4-x}Sn_xV_{0.6})O_{12}$($Sn_x$:Bi-CVG, x = 0.0, 0.2, 0.3, 0.4, 0.5, 0.6), were prepared by conventional ceramic technique. Appropriate amounts of raw materials, Y_2O_3(99.95%), Fe_2O_3(99.95%), Bi_2O_3(99.50%), SnO_2(99.99%), V_2O_5(99.00%), $CaCO_3$(99.50%), were mixed in a planetary ball mill with stainless steel ball and finally achieved an uniform mixture after milled for 4 h with deionized water. Afterwards, the mixture was dried, screened and calcined at 950 °C in air for 4 h, and then milled for 6 h with an average particle size of 2 μm. The obtained powders were pressed in a stainless-steel die under a pressure of 40,000 N/m^2 with 8 wt% polyvinyl-alcohol as a lubricant. Subsequently, the formed disks (30 mm diameter, 4.0–6.0 mm thickness) specimens were dried in an oven at 100 °C for 2 h and sintered in the temperature range 1000–1100 °C for 6 h. In order to carry out FMR measurements, the samples were spherically shaped by an abrasive technique capable of attaining sample diameters lower than 1 mm.

* Corresponding author. Tel.: +86 29 82201033; fax: +86 29 82202600.
E-mail address: xunnipy2006@126.com (N. Li).

0925-8388/$ – see front matter © 2011 Elsevier B.V. All rights reserved.
doi:10.1016/j.jallcom.2011.01.129

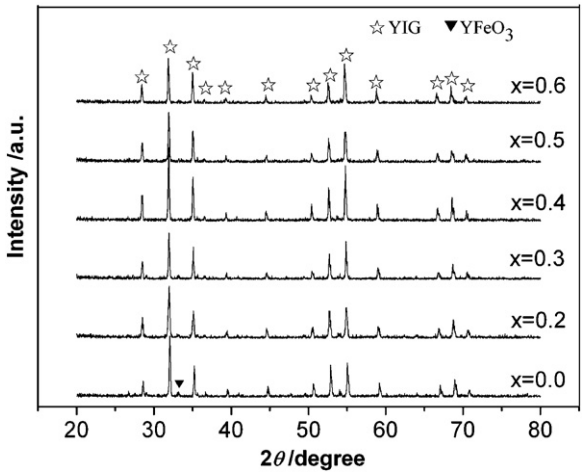

Fig. 1. XRD patterns of Sn_x:Bi-CVG specimens sintered at 1075 °C.

The density of the sintered garnet samples was measured using Archimedes method. The phase structures were determined by X-ray diffraction (XRD-7000S, Shimadzu Co., Tokyo, Japan, Cu Kα). The morphology and microstructure of the fracture surface were studied by a scanning electron microscope (SEM, JSM-6700F, JEOL Co., Tokyo, Japan). The B–H hysteresis loops of the materials were evaluated by measuring the impedance of a coil wound around the toroidal samples, with a Soft Magnetic Materials Automatic Test System (MATS, MATS-2010S, China) at room temperature with a field of 1600 A/m. Finally, the ferromagnetic resonance linewidth (ΔH) was measured with Microwave Ferrite Parameters Meter (ЭМ6-17M, Doman Co., Russia).

3. Results and discussion

3.1. Crystalline phase analysis

Fig. 1 shows the XRD patterns of the samples sintered at 1075 °C for 6 h. It is found that the samples exhibit mainly garnet phase with a smaller proportion of intermediate perovskite phase, $YFeO_3$. But the 2θ position of each crystal surface shows no difference at all with respect to the doping concentration of Sn^{4+}, implying that the substituting of Fe^{3+} with Sn^{4+} does not change the mainly crystal structure.

The lattice constants of the samples with different Sn concentrations (x) are shown in Fig. 2. It can be seen that the lattice constant increases monotonously with the Sn^{4+} content increasing. The ionic radius of Sn^{4+} (0.071 nm) is larger than that of Fe^{3+} (0.061 nm) on octahedral site of the garnet structure. Simultaneously, as a compensating charge, Ca^{2+} ion (0.112 nm) gets into dodecahedral site of the garnet structure instead of Y^{3+} ion whose ionic radius is relatively smaller (0.089 nm). Therefore, the lattice constant gradually increases with the Sn^{4+} content increasing.

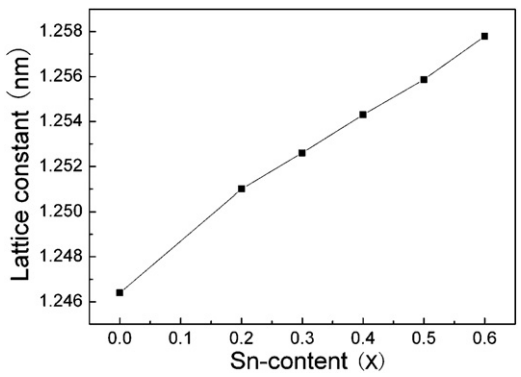

Fig. 2. Lattice constant of Sn_x:Bi-CVG specimens sintered at 1075 °C as a function of x.

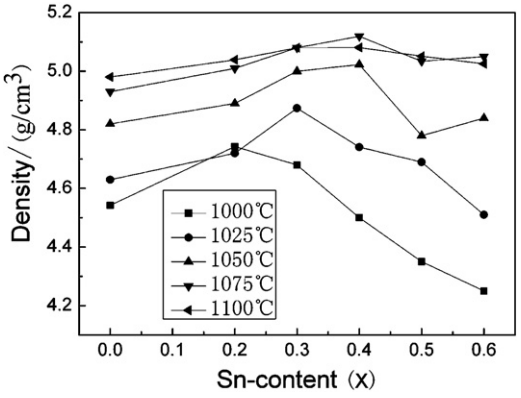

Fig. 3. Bulk density of Sn_x:Bi-CVG sintered at different temperatures.

Table 1
The theoretical density (TD) and relative density (RD) of Sn_x:Bi-CVG specimens at 1075 °C.

	x					
	0.0	0.2	0.3	0.4	0.5	0.6
TD (g/cm^3)	5.251	5.220	5.199	5.197	5.195	5.173
RD (%)	93.89	95.94	97.72	98.49	96.88	97.62

3.2. Density and structure characterization

Fig. 3 displays the bulk density of Sn_x:Bi-CVG sintered at different temperatures. The density of the specimens increases gradually with the sintering temperature as expected until higher than 1075 °C. Nevertheless, with further increase of the sintering temperature, the density does not significantly increase. Therefore, the optimum sintering temperature of Sn_x:Bi-CVG is about 1075 °C. In addition, under the same sintering temperature, the ceramic density first increases and then decreases with the Sn^{4+} content increasing. To explore the impact of Sn^{4+} on the density, the relative density (RD) and theoretical density (TD) of Sn_x:Bi-CVG sintered at 1075 °C are calculated and shown in Table 1. For the garnet structure, the theoretical density can be calculated by [3]

$$\rho = \frac{ZW_m}{N_A a_0^3} \quad (1)$$

where ρ is the theoretical density, Z the number of molecules per unit cell, W_m the molecular weight, N_A Avogadro constant and a_0 the lattice constant. Because that with the Sn^{4+} content increasing, the molecular weight W_m changes little and the lattice constant a_0 increases, the theoretical density decreases gradually. However, the bulk density increases at the beginning and then decreases. All these changes lead to the biggest relative density of 98.49% when $x = 0.4$.

Fig. 4 shows the SEM micrographs of $Sn_{0.4}$:Bi-CVG specimen with different sintering temperatures ranging from 1000 °C to 1100 °C. We can see that rising temperature increases the density and the grain size of the sample. But compared to Fig. 4(d), Fig. 4(e) shows the grain size is uniform, suggesting that the sintering temperature is too high. Therefore, we concluded that the optimal sintering temperature of $Sn_{0.4}$:Bi-CVG specimen is 1075 °C. In addition, substituting Fe^{3+} ion with Sn^{4+} can improve the microstructure of the sample.

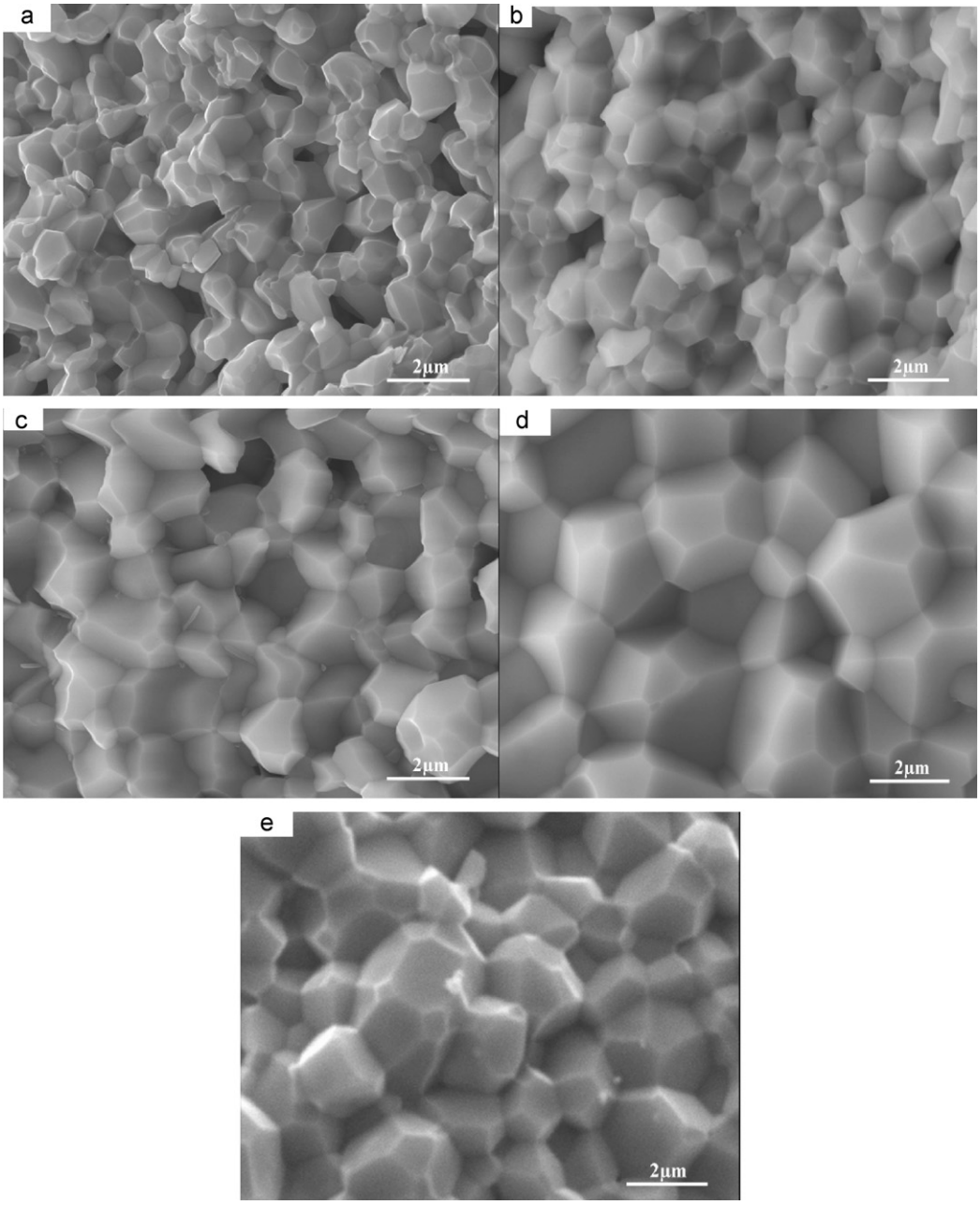

Fig. 4. SEM micrograph of $Sn_{0.4}$:Bi-CVG ferrite sintered at different temperatures: (a) 1000 °C, (b) 1025 °C, (c) 1050 °C, (d) 1075 °C, and (e) 1100 °C.

3.3. Magnetic properties

Fig. 5 displays the saturation magnetization (M_s) and the coercivity (H_c) of Sn_x:Bi-CVG specimens sintered at 1075 °C as a function of x. With x increasing to 0.4, M_S slowly increases, and H_c decreases. While x further increases, M_S sharply decreases and H_c slightly increases.

In the Bi-CVG crystal system, Bi^{3+}, Ca^{2+} and V^{5+} are non-magnetic ions while Fe^{3+} is magnetic ion. The magnetic moment caused by two Fe^{3+} ions in octahedral (*a*-) site is aligned anti-parallel to that caused by three Fe^{3+} ions in tetrahedral (*d*-) site, leaving a net magnetic moment from Fe^{3+} in the *d*-site. Therefore, M_S of Bi-CVG is given by the magnetic Fe^{3+} in the *d*-site. The total magnetic moment direction is consistent with the magnetic moment orientation of the Fe^{3+} ion in the *d*-site. Sn^{4+} belongs to non-magnetic ion and does not bring additional magnetic moment.

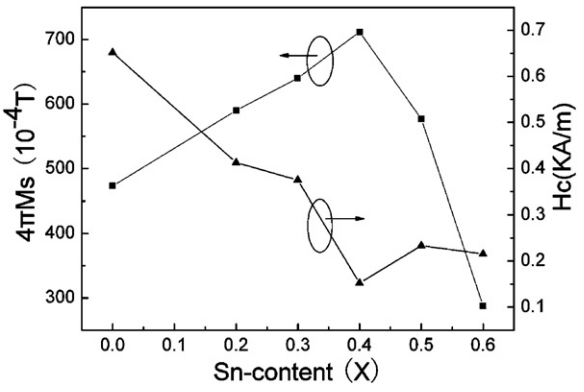

Fig. 5. Saturation magnetization (M_s) and the coercivity (H_c) of Sn_x:Bi-CVG specimens sintered at 1075 °C as a function of x.

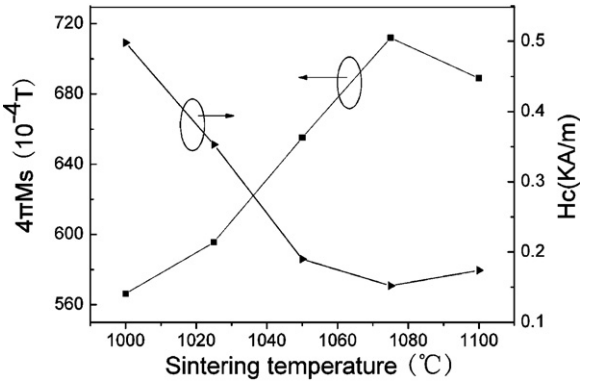

Fig. 6. Magnetic properties (M_s and H_c) of $Sn_{0.4}$:Bi-CVG with different sintering temperatures.

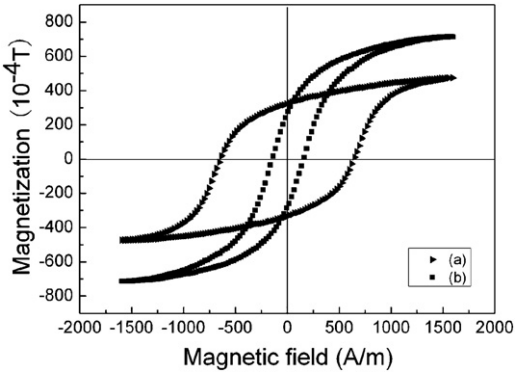

Fig. 7. Magnetic hysteresis loops (B–M_s curves) for Sn_x:Bi-CVG specimens of (a) $x = 0$ and (b) $x = 0.4$ at 1075 °C, respectively.

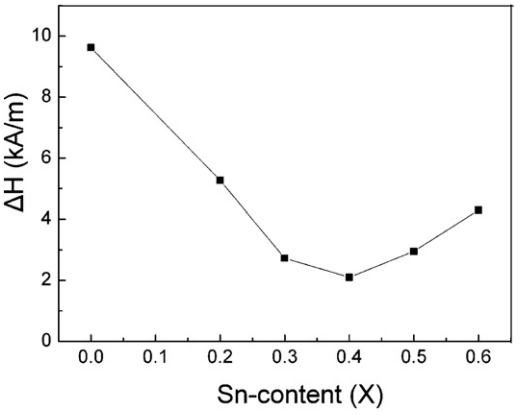

Fig. 8. Ferromagnetic resonance linewidth (ΔH) of Sn_x:Bi-CVG specimens sintered at 1075 °C as a function of x.

However, Sn^{4+} changes Fe^{3+} distributed condition between a-site and d-site in the garnet structure [18]. Sn^{4+} is inclined to occupy a-site, which causes that the quantity of Fe^{3+} in a-site reduces and then the net magnetic moment increases, thus M_s of ferrites strengthens. However, when the content of Sn^{4+} exceeds a critical point, due to too many non-magnetic ions in the a-site, a–d site super-exchange interaction becomes much weak, which causes the magnetic moments of partial Fe^{3+} ions in the d-site anti-parallel alignment, that is, magnetic moments with anti-parallel alignment in a–d site reduces, So the total magnetic moments no longer increase but reduce.

The coercive force H_c is determined by the magnetic domain wall motion and magnetic moment rotation [19]. For the garnet ferrite, its magnetic anisotropy constant K_1 is negative. Sn^{4+} ion replaces Fe^{3+} ion in a-site, Which reduces Fe^{3+} ion content in a-site and compensates negative anisotropy constant K_1 so that it approximates zero [20]. So the Sn^{4+} content x increases, magnetocrystalline anisotropy of ferrites decreases so that the resistance of domain wall motion and magnetic moment rotation reduces and thus H_c decreases. However, H_c slightly increases with $x > 0.4$, which may be due to the decrease of the density.

The magnetic properties (M_s and H_c) of $Sn_{0.4}$:Bi-CVG with different sintering temperatures are shown in Fig. 6. M_s increases with the sintering temperature increasing up to around 1075 °C, which is basically due to the increase of the density. Meanwhile, the average crystal grain increases and the distribution become more uniform (shown in Fig. 4), thus the ability of magnetic domain wall migration and magnetic moment rotation is enhanced, and so the coercive force H_c decreases. When the sintering temperature is higher than 1075 °C, the distribution of grain size is not uniform and the density slightly reduces, therefore, M_s slightly decreases and H_c slightly increases.

Fig. 7 shows the magnetic hysteresis loops (B–M_s curves) for Sn_x:Bi-CVG with $x = 0$ and $x = 0.4$. The values of saturation magnetization M_s and coercivity H_c of $x = 0.4$ specimen are 711.3×10^{-4} T and 152.3 A/m, respectively. Compared to $x = 0$ specimen, the saturation magnetization M_s increases by about 50.4% while the coercivity H_c decreases by about 76.7%. The results show that Sn^{4+} replacement obviously enhances the soft magnetic properties of Bi-CVG ferrite which sintered at low temperature as 1075 °C. Meanwhile, Compared to our previous result which is In-substituted Bi-CVG ceramic, the saturation magnetization M_s increases by about 40.5% while the coercivity H_c decreases by about 57.2%. So we replace In_2O_3 with SnO_2 which is cheap as raw material, leading to lower raw material costs and better magnetic properties.

3.4. Ferromagnetic resonance linewidth (ΔH)

Fig. 8 shows the X band (9.5 GHz) ferromagnetic resonance linewidth (ΔH) as a function of Sn^{4+} content at room-temperature. With x increasing, ΔH first sharply decreases, and then gradually increases when $x > 0.4$. The linewidth ΔH_a, caused by the fluctuations of magnetic anisotropy field due to the random orientation of grains, can be expressed as [21]:

$$\Delta H_a \approx \frac{2.07(K_1/M_s)^2}{M_s} \quad (2)$$

where K_1 is magnetic anisotropy constant. According to this equation, ΔH_a is inversely proportional to the cube of M_s. With x increasing, the saturation magnetization M_s first increases and then decreases, which causes ΔH_a contributing to ΔH to have the opposite trend. Meanwhile, the density of samples also influences the linewidth ΔH.

4. Conclusion

High density Sn_x:Bi-CVG ferrite samples were successfully prepared by conventional ceramic technique. The addition of SnO_2 could lower the sintering temperature and enhance the soft magnetic properties obviously. With the Sn^{4+} content increasing, the saturation magnetization M_s first increases and then decreases because Sn-substitution changes the superexchange interaction between a–d sites. While the coercivity H_c and the ferromagnetic resonance linewidth (ΔH) first sharply decrease and then slightly increase, which depend on both the magnetocrystalline anisotropy and the density. The specimen with $x = 0.4$ sintered at

1075 °C presents the best properties: RD = 98.49%, H_c = 152.3 A/m, $4\pi M_s = 711.3 \times 10^{-4}$ T, ΔH = 2.1 kA/m. Compared to the reported achievements in scientific research by conventional ceramic technique, the material has better properties at 1075 °C.

Acknowledgements

This work was supported by the Science and Technology Research Program funded projects of Shaanxi (Grant No. 07JC08) and Xi'an (Grant No. CXY08006).

References

[1] S. Mandal, S. Phadtare, Curr. Appl. Phys. 5 (2005) 118–127.
[2] J.W. Lee, J.H. Oh, J. Magn. Magn. Mater. 272–276 (2004) 2230–2232.
[3] T.C. Mao, J.C. Chen, J. Magn. Magn. Mater. 302 (2006) 74–81.
[4] E. Garskaite, K. Gibson, A. Leleckaite, J. Glaser, D. Niznansky, A. Kareiva, H.J. Meyer, Chem. Phys. 323 (2006) 204–210.
[5] T. Boudiar, B. Payet-Gervy, M.-F. Blanc-Mignon, J.-J. Rousseau, M. LeBerre, H. Joisten, J. Magn. Magn. Mater. 284 (2004) 77–85.
[6] C.Y. Tsay, C.Y. Liu, K.S. Liu, I.N. Lin, L.J. Hu, T.S. Yeh, J. Magn. Magn. Mater. 239 (2002) 490–494.
[7] F. Grasset, S. Mornet, J. Etourneau, H. Haneda, J.L. Bobet, J. Alloys Compd. 359 (2003) 330–337.
[8] L. Fernandez-Garcia, M. Suarez, J.L. Menendez, J. Alloys Compd. 502 (2010) 132–135.
[9] M. Niyaifar, A. Beitollahi, N. Shiri, M. Mozaffari, J. Amighian, J. Magn. Magn. Mater. 322 (2010) 777–779.
[10] R.J. Young, T.B. Wu, I.N. Lin, J. Mater. Sci. 25 (1990) 3566–3572.
[11] C.Y. Tsay, C.Y. Liu, K.S. Liu, I.N. Lin, L.J. Hu, T.S. Yeh, Mater. Chem. Phys. 79 (2003) 138–142.
[12] S. Geller, H.J. Williams, G.P. Espinosa, R.C. Sherwood, M.A. Gilleo, Appl. Phys. Lett. 3 (2) (1963) 21.
[13] K. Shinagawa, S. Taniguchi, Jpn. J. Appl. Phys. 12 (3) (1973) 465.
[14] Y.Y. Song, S.C. Yu, W.T. Kim, J.R. Park, T.H. Kim, J. Magn. Magn. Mater. 177–181 (1998) 257.
[15] S. Geller, G.P. Espinosa, H.J. Williams, R.C. Sherwood, E.A. Nesbitt, Appl. Phys. Lett. 35 (1964) 570.
[16] L.R. Hodges, G.P. Rodrigue, G.R. Harrison, A.D. Sanders, J. Appl. Phys. 37 (1966) 1085.
[17] Q.M. Xu, W.B. Liu, L.J. Hao, C.J. Gao, X.G. Lu, Y.A. Wang, J.S. Zhou, J. Magn. Magn. Mater. 322 (2010) 2276–2280.
[18] Guo-Dong Li, Rare Metal Mater. Eng. 35 (2) (2006) 169–171.
[19] A. Globus, P. Duplex, IEEE Trans. Magn. 7 (3) (1971) 617–621.
[20] Zhi-Gang Zhou, Ferrite Magnetic Materials [M], Science Press, Beijing, February 1981, pp. 555–558.
[21] E. Schlomann, J. Phys. Chem. Sol. 6 (1958) 242–254.